New Carbazole−Oxadiazole Dyads for Electroluminescent Devices: Influence of Acceptor Substituents on Luminescent and Thermal Properties

K. R. Justin Thomas,[†] Jiann T. Lin,*[,†,‡] Yu-Tai Tao,*[,†] and Chang-Hao Chuen[†]

Institute of Chemistry, Academia Sinica, 115 Nankang, Taipei, Taiwan, Republic of China, and Department of Chemistry, National Central University, 320 Chungli, Taiwan, Republic of China

Received July 24, 2004. Revised Manuscript Received September 29, 2004

A series of carbazole−oxadiazole dyads linked by amino functionality is prepared in good yields by C−N coupling reactions catalyzed by $Pd(dba)_2/P(t\text{-}Bu)_3$ under basic conditions in toluene. The compounds possess additional electron-withdrawing groups such as CF_3 and CN either on oxadiazole or on carbazole nucleus. The placement of CF_3 on the oxadiazole end enhances the electron deficiency of the oxadiazole unit, while the CN substituent at the carbazole nucleus decreases the donor strength of carbazole. This results in slight alterations in the oxidation potentials and thermal properties of the resulting dyads. This also leads to a pathway for fine-tuning the energy levels and amorphous morphology in these dyads. While CN groups alter by ~0.2 eV the energy levels, a counterproductive T_g reduction/thermal instability is observed for the CF_3 derivatives. All of these derivatives display solvent-dependent emission profiles with the solid-state emission occurring in the cyan region. Electroluminescent devices fabricated using these compounds as hole-transporting layer and Alq_3 or TPBI as the electron-transporting layer emit cyan color. The emission in most cases arises from the HTL layer. However, slight distortions in shape and peak position of the EL spectra were noticed, which were attributed to either the mixing of emissions from HTL and ETL layer or the complex formation between the HTL and ETL materials. Energetics governing the confinement of excitons in the emissive layer is critically analyzed.

Introduction

Materials suitable for application in organic light-emitting diodes have been actively researched in the past decade because of their potential application in flat-panel displays and the academic interest on the structure−property relationship of molecules featuring multiple functional moieties.[1,2] Generally, functional materials are prepared in various structural forms such as small molecules, dendrimers, and polymers. In small molecules and dendrimers, precise control could be achieved on the orientation of the functional groups and thus the resulting properties. For an effective function in an electroluminescent device, a molecule must possess hole/electron transport, bright emission with sharp color chromaticity, and stable thermal characteristics.[3] Dipolar compounds with emission characteristics are ideal for this purpose as they will inherit the propensity for the stabilization of both positive and negative charges.[4,5] This will eventually balance and streamline the passage of holes/electrons within the molecular layer and effectively produce excitons that finally result in bright emission. The use of such triple functional molecules will eliminate the cumbersome and multistep layer-by-layer fabrication process and also will be cost-effective.

Bipolar formant character has been reported in dyads featuring triarylamine−oxadiazole,[4−7] carbazole−quinoxaline,[8] triarylamine−pyridine/quinoline,[9,10] and triarylamine−diarylboron[11,12] architectures. Dipolar molecules tend to form the crystalline state, partially due to the planar structure and the $\pi-\pi$ stacking interaction

* Corresponding author. Fax: Int. code +(2)27831237. E-mail: jtlin@chem.sinica.edu.tw.

† Academia Sinica.

‡ National Central University.

(1) (a) Sheats, J. R.; Antoniadis, H.; Hueschen, M.; Leonard, W.; Miller, J.; Moon, R.; Roitman, D.; Stocking, A. *Science* **1996**, *273*, 884. (b) Gross, M.; Muller, D. C.; Nothofer, H. G.; Scherf, U.; Neher, D.; Brauchle, C.; Meerholz, K. *Nature* **2000**, *405*, 661.

(2) (a) Hung, L. S.; Chen, C. H. *Mater. Sci. Eng. Rep*. **2002**, *39*, 143. (b) Shim, H. K.; Jin, J. I. *Adv. Polym. Sci*. **2002**, *158*, 193. (c) Muller, C. D.; Falcou, A.; Reckefuss, N.; Rojahn, M.; Wiederhirn, V.; Rudati, P.; Frohne, H.; Nuyken, O.; Becker, H.; Meerholz, K. *Nature* **2003**, *421*, 829. (d) Slinker, J.; Bernards, D.; Houston, P. L.; Abruna, H. D.; Bernhard, S.; Malliaras, G. G. *Chem. Commun.* **2003**, 2392. (e) Akcelrud, L. *Prog. Polym. Sci*. **2003**, *28*, 875.

(3) Mitschke, U.; Bäuerle, P. *J. Mater. Chem*. **2000**, *10*, 1471. Segura, J. L. *Acta Polym*. **1998**, *49*, 319.

(4) Shu, C. F.; Dodda, R.; Wu, F. I.; Liu, M. S.; Jen, A. K. Y. *Macromolecules* **2003**, *36*, 6698.

(5) (a) Guan, M.; Bian, Z. Q.; Zhou, Y. F.; Li, F. Y.; Li, Z. J.; Huang, C. H. *Chem. Commun*. **2003**, 2708. (b) Chan, L. H.; Lee, R. H.; Hsieh, C. F.; Yeh, H. C.; Chen, C. T. *J. Am. Chem. Soc*. **2002**, *124*, 6469. (c) Yeh, H. C.; Lee, R. H.; Chan, L. H.; Lin, T. Y. J.; Chen, C. T.; Balasubramaniam, E.; Tao, Y.-T. *Chem. Mater*. **2001**, *13*, 2788.

(6) (a) Mochizuki, H.; Hasui, T.; Kawamoto, M.; Shiono, T.; Ikeda, T.; Adachi, C.; Taniguchi, Y.; Shirota, Y. *Chem. Commun*. **2000**, 1923. (b) Tamoto, N.; Adachi, C.; Nagai, K. *Chem. Mater*. **1997**, *9*, 1077.

(7) (a) Mochizuki, H.; Hasui, T.; Kawamoto, M.; Ikeda, T.; Adachi, C.; Taniguchi, Y.; Shirota, Y. *Macromolecules* **2003**, *36*, 3457. (b) Peng, Z. H.; Bao, Z. N.; Galvin, M. E. *Chem. Mater.* **1998**, *10*, 2086.

10.1021/cm048794u CCC: $27.50 © 2004 American Chemical Society
Published on Web 11/16/2004

between the aromatic moieties. Additionally, dipole alignments also leads to long-range ordered structures. Even though the triarylamine−oxadiazole derivatives have been found to exhibit amorphous behavior, they form crystals at higher temperatures. Attempts have been made to tune the morphology of the electroluminescent materials by varying the structural elements.[13] However, to the best of our knowledge, tuning the functional properties of the carbazole−oxadiazole conjugates by tethering additional electron-withdrawing groups has not been demonstrated.

Earlier, we reported a series of carbazole-based small molecules featuring pyrene and found that they effectively function as hole-transport and emitting materials in OLEDs.[14−16] Later, we demonstrated that incorporation of oxadiazole and quinoxaline electron-withdrawing segments in the structural motifs effectively confined the holes and electrons inside the molecular layer.[17] We have also established recently that incorporation of CN groups on the carbazole nucleus significantly alters the energy levels of the carbazolylamines and leads to efficient electroluminescent devices when such molecules are used as the hole-transporting layer.[18] This we attributed to the retardation of the hole mobility while facilitating the electron mobility in the HTL layer. In this Article, we report a series of compounds that contain both carbazole and oxadiazole functional moieties. In addition, we incorporate small electron-withdrawing groups such as CN and CF_3 and explore their role in the operation of OLEDs.

Experimental Section

General Information. Unless otherwise specified, all reactions and manipulations were performed under nitrogen atmosphere using standard Schlenk techniques. All chromatographic separations were carried out on silica gel (60 M, 230−400 mesh). Dichloromethane and dimethylformamide (DMF) were distilled from calcium hydride under nitrogen atmosphere. Other solvents were purified by routine procedures. ^{1}H spectra were recorded on a Bruker AC300 spectrometer operating at 300.135. Mass spectra (FAB) were recorded on a Hewlett-Packard GC/MS 5995 spectrometer. Elemental analyses were performed on a Perkin-Elmer 2400 CHN analyzer. Electronic absorption spectra were measured on a Cary 50 Probe UV−visible spectrometer. Emission spectra were recorded by a Hitachi fluorescence spectrometer (F4500). Emission quantum yields were obtained by standard method[19] using Coumarin-I as reference. Cyclic voltammetry experiments were performed with a BAS-100 electrochemical analyzer. All measurements were carried out at room temperature with a conventional three-electrode configuration consisting of a glassy carbon working electrode, platinum auxiliary electrode, and a nonaqueous $Ag/AgNO_3$ reference electrode. The $E_{1/2}$ values were determined as $1/2(E_p^a + E_p^c)$, where E_p^a and E_p^c are the anodic and cathodic peak potentials, respectively. All potentials reported are not corrected for the junction potential. The solvent in all experiments was CH_2Cl_2, and the supporting electrolyte was 0.1 M tetrabutylammonium hexafluorophosphate. DSC measurements were carried out on a Perkin-Elmer differential scanning calorimeter at a heating rate of 10 °C/min and a cooling rate of 30 °C/min under nitrogen atmosphere. TGA measurements were performed on a TA-7 series thermogravimetric analyzer at a heating rate of 10 °C/min under a flow of air. 6-Bromo-9-ethyl-9*H*-carbazole-3-carbonitrile was available from an earlier study.[16]

9-Ethyl-6-phenylamino-9*H*-carbazole-3-carbonitrile. 6-Bromo-9-ethyl-9*H*-carbazole-3-carbonitrile (2.99 g, 10 mmol), aniline (1.40 g, 15 mmol), potassium *tert*-butoxide (1.44 g, 15 mmol), $Pd(dba)_2$ (95 mg), $(t\text{-Bu})_3P$ (0.02−0.04 mmol), and toluene (20 mL) were mixed together and heated at 80 °C for 12 h. After being cooled, the reaction was quenched by the addition of water and extracted with diethyl ether (3 × 50 mL). The combined organic extract was dried over anhydrous $MgSO_4$ and evaporated to dryness to yield a tan solid. It was adsorbed on silica gel and purified by column chromatography. The desired compound was eluted with dichloromethane: hexane (3:2) mixtures. Yield: 2.89 g (93%). Colorless solid. FAB MS: *m/z* 311 (M^+). ^{1}H NMR ($CDCl_3$): δ 1.42 (t, J = 7.3 Hz, 3H), 4.51 (q, J = 7.3 Hz, 2H), 6.75−6.81 (m, 1H), 7.08 (d, 8.1 Hz, 2H), 7.17−7.23 (m, 2H), 7.40 (dd, J = 8.5, 2.1 Hz, 1H), 7.59 (d, J = 8.1 Hz, 1H), 7.67−7.74 (m, 2H), 8.06 (d, J = 2.1 Hz, 1H), 8.56 (s, 1H).

(9-Ethyl-9*H*-carbazol-3-yl)-*p*-tolyl-amine. This was prepared from 3-bromo-9- ethyl-9*H*-carbazole and *p*-toluidine following the method as described above in 89% yield. FAB MS: *m/z* 300 (M^+). ^{1}H NMR ($CDCl_3$): δ 1.38 (t, J = 7.3 Hz, 3H), 2.23 (s, 3H), 4.43 (q, J = 7.3 Hz, 2H), 6.94−7.02 (m, 4H), 7.13 (t, J = 7.6 Hz, 1H), 7.28 (dd, J = 8.1, 2.1 Hz, 1H), 7.39−7.52 (m, 3H), 7.89 (d, J = 2.1 Hz, 1H), 8.05 (d, J = 8.1 Hz, 1H).

{4-[5-(4-*tert*-Butyl-phenyl)-[1,3,4]oxadiazol-2-yl]-phenyl}-(9-ethyl-9*H*-carbazo l-3-yl)-phenyl-amine (compound **1**) was described in an earlier report.[17] Compounds **2**−**6** were obtained by essentially following a procedure similar to that described above from the corresponding precursors.

(9-Ethyl-9*H*-carbazol-3-yl)-phenyl-{4-[5-(4-trifluoromethyl-phenyl)-[1,3,4]oxadiazol-2-yl]-phenyl}-amine (2). Yellow solid. Yield: 76%. FAB MS: *m/z* 575 (M^+). ^{1}H NMR ($CDCl_3$): δ 1.46 (t, J = 7.3 Hz, 3H), 4.37 (q, J = 7.3 Hz, 2H), 7.09−7.12 (m, 3H), 7.19 (t, J = 9.0 Hz, 1H), 7.23−7.49 (m, 8H), 7.64 (t, J = 7.8 Hz, 1H), 7.76 (d, J = 7.8 Hz, 1H), 7.92−7.99 (m, 4H), 8.29 (d, J = 7.8 Hz, 1H), 8.35 (s, 1H). Anal. Calcd for $C_{35}H_{25}F_3N_4O$: C, 73.16; H, 4.39; N, 9.75. Found: C, 73.04; H, 4.21; N, 9.82.

{4-[5-(4-*tert*-Butyl-phenyl)-[1,3,4]oxadiazol-2-yl]-phenyl}-(9-ethyl-9*H*-carbazol-3-yl)-*p*-tolyl-amine (3). Yellow solid. Yield: 89%. FAB MS: *m/z* 577 (M^+). ^{1}H NMR ($CDCl_3$): δ 1.35 (s, 9H), 1.45 (t, J = 7.3 Hz, 3H), 2.32 (s, 3H), 4.50 (q, J = 7.3 Hz, 2H), 7.01 (d, J = 8.8 Hz, 2H), 7.14−7.19 (m, 5H), 7.3 (dd, J = 8.8, 2.1 Hz, 1H), 7.47 (t, J = 8.8 Hz, 1H), 7.57−7.65 (m, 4H), 7.91 (d, J = 8.8 Hz, 2H), 8.02−8.11 (m, 6H). Anal. Calcd for $C_{39}H_{36}N_4O$: C, 81.22; H, 6.29; N, 9.71. Found: C, 81.14; H, 6.07; N, 9.66.

(9-Ethyl-9*H*-carbazol-3-yl)-*p*-tolyl-{4-[5-(4-trifluoromethyl-phenyl)-[1,3,4]oxadiazol-2-yl]-phenyl}-amine (4). Yel-

(8) (a) Justin Thomas, K. R.; Lin, J. T.; Tao, Y.-T.; Chien, C. H. *Chem. Mater.* **2002**, *14*, 2796. (b) Justin Thomas, K. R.; Lin, J. T.; Tao, Y.-T.; Chien, C. H. *J. Mater. Chem.* **2002**, *12*, 3516. (c) Wang, P. F.; Xie, Z. Y.; Wong, O. Y.; Lee, C. S.; Wong, N. B.; Hung, L. S.; Lee, S. T. *Chem. Commun.* **2002**, 1404. (d) Wang, P. F.; Xie, Z. Y.; Hong, Z. R.; Tang, J. X.; Wong, O. Y.; Lee, C. S.; Wong, N. B.; Lee, S. T. *J. Mater. Chem.* **2003**, *13*, 1894.

(9) Tao, Y.-T.; Chuen, C.-H.; Ko, C.-W.; Peng, J.-W. *Chem. Mater.* **2002**, *14*, 4256. Wang, Y. Z.; Epstein, A. J. *Acc. Chem. Res.* **1999**, *32*, 217 and references therein.

(10) Jenekhe, S. A.; Lu, L. D.; Alam, M. M. *Macromolecules* **2001**, *34*, 7315.

(11) (a) Shirota, Y.; Kinoshita, M.; Noda, T.; Okumoto, K.; Ohara, T. *J. Am. Chem. Soc.* **2000**, *122*, 11021. (b) Doi, H.; Kinoshita, M.; Okumoto, K.; Shirota, Y. *Chem. Mater.* **2003**, *15*, 1080.

(12) Mutaguchi, D.; Okumoto, K.; Ohsedo, Y.; Moriwaki, K.; Shirota, Y. *Org. Electron.* **2003**, *4*, 49.

(13) Shirota, Y. *J. Mater. Chem.* **2000**, *10*, 1.

(14) Justin Thomas, K. R.; Lin, J. T.; Tao, Y.-T.; Ko, C.-W. *Adv. Mater.* **2000**, *12*, 1949.

(15) Justin Thomas, K. R.; Lin, J. T.; Tao, Y.-T.; Ko, C.-W. *J. Am. Chem. Soc.* **2001**, *123*, 9405.

(16) Kundu, P.; Justin Thomas, K. R.; Lin, J. T.; Tao, Y.-T.; Chien, C. H. *Adv. Funct. Mater.* **2003**, *134*, 445.

(17) Justin Thomas, K. R.; Lin, J. T.; Tao, Y.-T.; Chien, C. H. *Chem. Mater.* **2002**, *14*, 3852.

(18) Justin Thomas, K. R.; Velusamy, M.; Lin, J. T.; Tao, Y.-T.; Chien, C. H. *Adv. Funct. Mater.* **2004**, *14*, 387.

(19) Demas, J. N.; Crosby, G. A. *J. Phys. Chem.* **1971**, *75*, 991.

Scheme 1

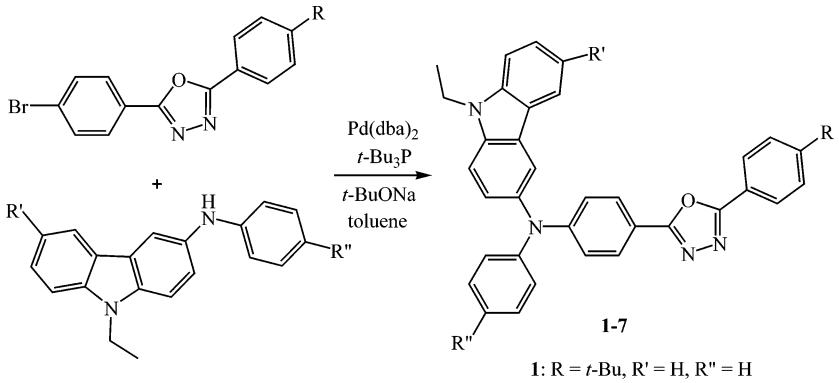

1-7

1: R = *t*-Bu, R' = H, R" = H
2: R = CF_3, R' = H, R" = H
3: R = *t*-Bu, R' = H, R" = Me
4: R = CF_3, R' = H, R" = Me
5: R = *t*-Bu, R' = CN, R" = H
6: R = CF_3, R' = CN, R" = H

low solid. Yield: 92%. FAB MS: *m/z* 589 (M^+). ^{1}H NMR ($CDCl_3$): δ 1.46 (t, 7.3 Hz, 3H), 2.34 (s, 3H), 4.36 (q, J = 7.3 Hz, 2H), 7.04 (d, J = 8.8 Hz, 2H), 7.14−7.20 (m, 5H), 7.30 (d, J = 8.8 Hz, 1H), 7.37−7.49 (m, 3H), 7.64 (t, J = 8.8 Hz, 1H), 7.76 (d, J = 8.8 Hz, 1H), 7.88−7.98 (m, 4H), 8.29 (d, J = 8.8 Hz, 1H), 8.34 (s, 1H). Anal. Calcd for $C_{36}H_{27}F_3N_4O$: C, 73.46; H, 4.62; N, 9.52. Found: C, 73.41; H, 4.50; N, 9.38.

6-({4-[5-(4-*tert*-Butyl-phenyl)-[1,3,4]oxadiazol-2-yl]-phenyl}-phenyl-amino)-9-ethyl-9*H*-carbazole-3-carbonitrile (5). Yellow solid. Yield: 95%. FAB MS: *m/z* 588 (M^+). ^{1}H NMR ($CDCl_3$): δ 1.34 (s, 9H), 1.48 (t, J = 7.3 Hz, 3H), 4.38 (q, J = 7.3 Hz, 2H), 7.06−7.13 (m, 3H), 7.19 (d, J = 8.8 Hz, 2H), 7.29−7.34 (t, J = 8.8 Hz, 2H), 7.38−7.45 (m, 3H), 7.51 (d, J = 8.8 Hz, 2H), 7.68 (dd, J = 8.8, 2.1 Hz, 1H), 7.90−7.94 (m, 3H), 7.81 (d, J = 8.8 Hz, 2H), 8.27 (s, 1H). Anal. Calcd for $C_{39}H_{33}N_5O$: C, 79.70; H, 5.66; N, 11.92. Found: C, 79.63; H, 5.49; N, 11.84.

9-Ethyl-6-(phenyl-{4-[5-(4-trifluoromethyl-phenyl)-[1,3,4]-oxadiazol-2-yl]-phenyl}-amino)-9*H*-carbazole-3-carbonitrile (6). Yellow solid. Yield: 85%. FAB MS: *m/z* 600 (M^+). ^{1}H NMR ($CDCl_3$): δ 1.48 (t, J = 7.3 Hz, 3H), 4.39 (q, J = 7.3 Hz, 2H), 7.07−7.15 (m, 3H), 7.21 (d, J = 8.8 Hz, 2H), 7.3−7.36 (m, 2H), 7.38−7.46 (m, 2H), 7.62−7.70 (m, 2H), 7.77 (d, J = 7.9 Hz, 1H), 7.94 (d, J = 8.9 Hz, 3H), 8.27−8.33 (m, 3H). Anal. Calcd for $C_{36}H_{24}F_3N_5O$: C, 72.11; H, 4.03; N, 11.68. Found: C, 72.06; H, 3.93; N, 11.51.

OLED Fabrication and Measurements. Electron-transporting materials TPBI (1,3,5-tris(*N*-phenylbezimidazol-2-yl)-benzene)[20] and Alq_3 (tris(8-hydroxyquinoline) aluminum)[21] were synthesized according to literature procedures and were sublimed twice prior to use. Prepatterned ITO substrates with an effective individual device area of 3.14 mm^2 were cleaned as described in a previous report.[22] Double-layer EL devices using carbazole derivatives as the hole-transport layer and TPBI or Alq_3 as the electron-transport layer were fabricated. For comparison, a typical device using NPB (1,4-bis(1-naphthylphenylamino)biphenyl) as the hole-transporting layer was also prepared. All devices were prepared by vacuum deposition of 400 Å of the hole-transporting layer (compounds **2**−**6**), followed by 400 Å of TPBI or Alq_3. An alloy of magnesium and silver (ca. 10:1, 500 Å) was deposited as the cathode, which was capped with 1000 Å of silver. I−V curve was measured on a Keithley 2400 source meter in an ambient environment. Light intensity was measured with a Newport 1835 optical meter.

Results and Discussion

Synthesis and Characterization. The synthesis of the oxadiazole-incorporated carbazolylamines (**2**−**6**) was achieved by the palladium catalyzed C−N coupling reactions[23] involving $Pd(dba)_2$/P(*t*-Bu)$_3$ catalyst and *t*-BuONa base (Scheme 1). The reactions occurred at room temperature. However, increasing the reaction temperature to 80 °C led to the fast completion of the reaction. Typical yields ranged from 75% to 95%. The compounds are pale yellow in color and soluble in most organic solvents but insoluble in alcohols. The compounds were purified by reprecipitating twice from dichloromethane/methanol mixtures prior to application in electroluminescent devices. The ^{1}H NMR spectra recorded in $CDCl_3$ and mass spectral data are in accordance with the structure of the molecules.

Optical Properties. The absorption and emission spectra of the compounds were investigated in dichloromethane and toluene solutions, and the pertinent data are listed in Table 1. No solvatochromism in the absorption spectra was observed. However, existence of a strong dipole in the excited state of the molecule was evidenced by the red shift of the fluorescence maxima in the dichloromethane solutions when compared to the toluene solutions. The absorption and emission spectra of the CF_3 substituted compounds (**2**, **4**, and **6**) are displayed in Figure 1. An intense absorption band around 360 nm attributed to the charge-transfer transition is noticed in all of the compounds. Within a series (CF_3 or *tert*-butyl), the wavelength of this absorption band adopts the following trend: **6** < **2** < **4** (**5** < **1** < **3**). A similar trend is also discernible in the emission data. A strong blue shift observed for the CN-substituted compounds is intriguing. This may be rationalized as below. An electron-rich substituent at the phenylamine (methyl in **3** and **4**) connected with the oxadiazole moiety leads to a slightly strong dipolar interaction as it enhances the electron-richness of the amine. However, the presence of a CN on the carbazole nucleus (in **5** and **6**) diminishes the donor capacity of the carbazole and

(20) Shi, J.; Tang, C. W.; Chen, C. H. U.S. Patent, 5,645,948, 1997. Sonsale, A. Y.; Gopinathan, S.; Gopinathan, C. *Indian J. Chem.* **1976**, *14*, 408.

(21) Chen, C. H.; Shi, J.; Tang, C. W. *Coord. Chem. Rev.* **1998**, *171*, 161.

(22) Wu, I.-Y.; Lin, J. T.; Tao, Y.-T.; Balasubramaniam, E.; Su, Y.-Z.; Ko, C.-W. *Chem. Mater.* **2001**, *13*, 2626.

(23) (a) Hartwig, J. F. *Synlett* **1997**, 329−340. Hartwig, J. F. *Angew. Chem., Int. Ed.* **1998**, *37*, 2046. (b) Hartwig, J. F. *Acc. Chem. Res.* **1998**, *31*, 852. (c) Hartwig, J. F.; Kawatsura, M.; Hauck, S. I.; Shaughnessy, K. H.; Alcazar-Roman, L. M. *J. Org. Chem.* **1999**, *64*, 5575.

Table 1. Optical, Thermal, and Electrochemical Data of the Compounds[a]

compd	λ_{abs}, nm	λ_{em},[b] nm	Φ_f, %	E_{ox} (ΔE_p), mV	HOMO, eV	LUMO, eV	T_g, °C	T_d, °C
2	373	484 (546, 508)	63	339 (83), 862(80)	5.1	2.3	85	380
3	367	471 (526, 494)	46	295 (117), 848 (124)	5.1	2.2	110	405
4	375	491 (554, 512)	53	300 (78), 837 (77)	5.1	2.3	90	370
5	362	446 (495, 474)	50	450 (105), 991 (87)	5.3	2.3	129	425
6	369	460 (514, 490)	66	463 (88), 994 (77)	5.3	2.4	104	400
1[c]	367	467 (520, 490)	22	322 (88), 851 (81)	5.1	2.2	106	415

[a] Absorption and emission spectra were recorded for toluene solutions. Quantum yield was measured with reference to Coumarin-I (99%) in ethyl acetate. Refractive index change due to the use of different solvent correction was applied in the calculation. Oxidation potential reported is adjusted to the potential of ferrocene, which was used as an internal reference. Conditions of cyclic voltammetric measurements: glassy carbon working electrode; $Ag/AgNO_3$ reference electrode. Scan rate: 100 mV/s. Electrolyte: tetrabutylammonium hexafluorophosphate. Decomposition temperature (T_d) corresponds to the 5% weight loss. HOMO calculated from CV potentials using ferrocene as standard [HOMO = 4.8 + ($E_{ox} - E_{Fc}$)]. LUMO derived from the relationship E_g = HOMO − LUMO, where E_g was obtained from optical spectroscopy. [b] Emission maxima observed for dichloromethane solutions and film are provided in the parentheses. [c] Data taken from ref 17.

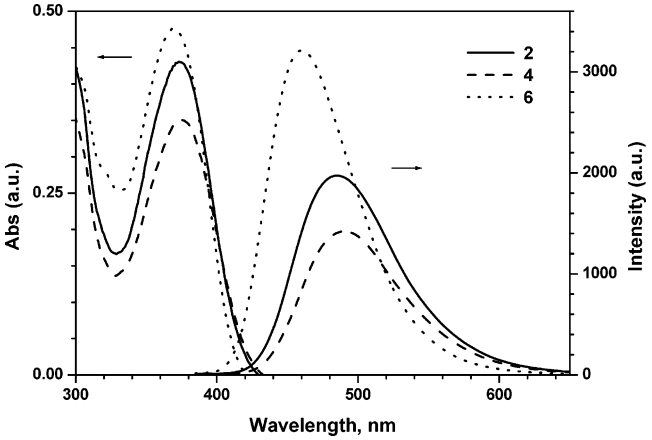

Figure 1. Absorption and emission spectra of compounds **2**, **4**, and **6** in toluene solutions.

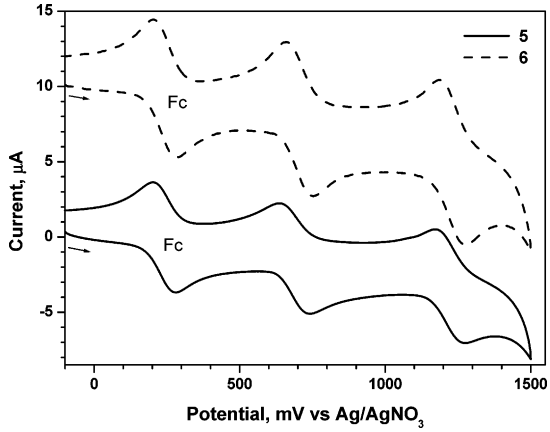

Figure 2. Cyclic voltammograms of compounds **5** and **6** recorded in dichloromethane solutions (scan rate 100 mV/s).

thus the 6-amino unit. This effect is also observed in the oxidation propensity of the amines as inferred from the cyclic voltammetry results (vide infra).

All of the compounds emit blue to green colors in toluene solutions with moderate quantum yields. The quantum yield drops substantially when measured in CH_2Cl_2. As observed in dichloromethane solution (vide supra), the emission profile exhibits a red shift when recorded as a film. These alterations in emission characteristics more likely stem from the dipolar interactions with the polar solvents and in the solid state probably from the intermolecular interactions which could increase the effective conjugation in the solid state.

Electrochemical Properties. The redox nature of the compounds was examined by the cyclic voltammetry in dichloromethane solutions. All of the compounds exhibit two quasi-reversible oxidation waves at potentials higher than that observed for ferrocene. The first less-positive oxidation potential is attributed to the electron removal from the peripheral amine. This displays a slight anodic shift (5−17 mV) for the CF_3-substituted compounds when compared to the *tert*-butyl-substituted analogues. However, the influence of CN substitution on carbazole nucleus (compare **5** and **6** with **1** and **2**) and methyl insertion on phenyl moiety (compare **3** and **4** with **1** and **2**) is more dramatically felt on the first oxidation potential. Consequently, the tolyl-substituted compounds (**3** and **4**) show the lowest oxidation potentials, while the CN-substituted analogues (**5** and **6**) display the most anodic oxidation waves (Figure 2). The above observations clearly point that the electron-deficient CF_3 group enhances the electron-withdrawing ability of the oxadiazole unit and the CN group suppresses the electron-donating strength of the carbazole nucleus. Fluorine substitution was earlier found to be instrumental in raising the oxidation potential of the polyphenylene polymer.[24] It must be noted that donor groups attached to an amine will increase the oxidation propensity of the amine while an opposite effect will be operative if an electron-deficient group is linked to the amine.

A similar substituent effect is observed in the second oxidation wave attributable to the carbazole unit. The influence of the CN group is more prominent due to the anchoring of the CN directly on the carbazole unit.

Thermal Properties. All of the compounds are amorphous in nature. They exhibit moderate glass transition temperatures in the range 85−129 °C which is higher than that recorded for the commonly used hole-transporting agent TPD. The CF_3-substituted deriva-

(24) (a) Riehn, R.; Morgado, J.; Iqbal, R.; Moratti, S. C.; Holmes, A. B.; Volta, S.; Cacialli, F. *Synth. Met.* **2001**, *124*, 67. (b) Riehn, R.; Morgado, J.; Iqbal, R.; Moratti, S. C.; Holmes, A. B.; Volta, S.; Cacialli, F. *Macromolecules* **2000**, *33*, 3337.

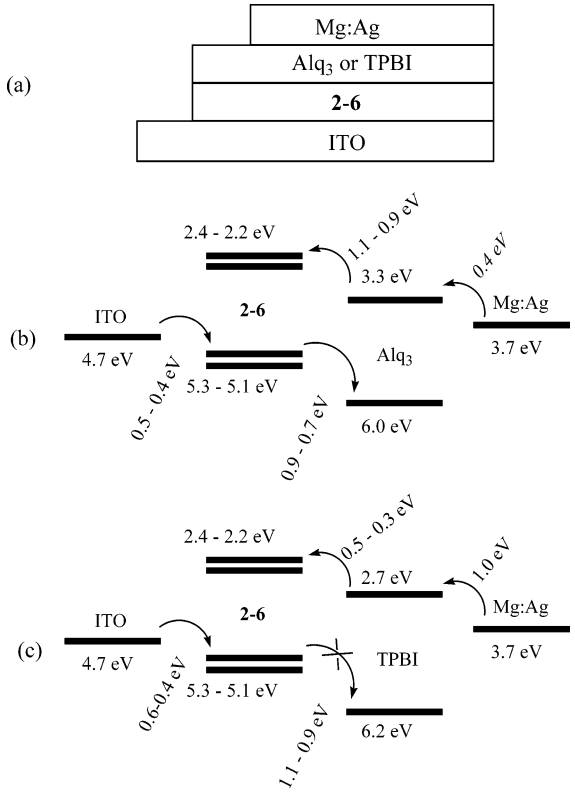

Figure 3. Cross-sectional view of the devices (a) and energy alignment of the constituents in the Alq_3 (b)- and TPBI (c)-based devices.

tives (**2**, **4**, and **6**) display lower T_g values when compared to the corresponding *tert*-butyl analogues (**1**, **3**, and **5**). The CN derivatives show a large variation (25 °C) between the CF_3 and *tert*-butyl derivatives (compare **5** and **6**). A similar effect is also observed in the thermal stability. Thus, in general, the thermal stability of the trifluoromethyl (**2**, **4**, and **6**)-substituted compounds is inferior to that of the *tert*-butyl derivatives (**1**, **3**, and **5**). Within the series, the T_g is in the order **6** > **4** > **2** (**5** > **3** > **1**). Yet the order in thermal stability is slightly different: **6** > **2** > **4** (**5** > **1** > **3**). Facile decomposition in the tolylamino derivatives (**3** and **4**) is probably triggered by the loss of the methyl moieties. Similarly, the origin of instability in compounds **2**, **4**, and **6** is the CF_3 unit.

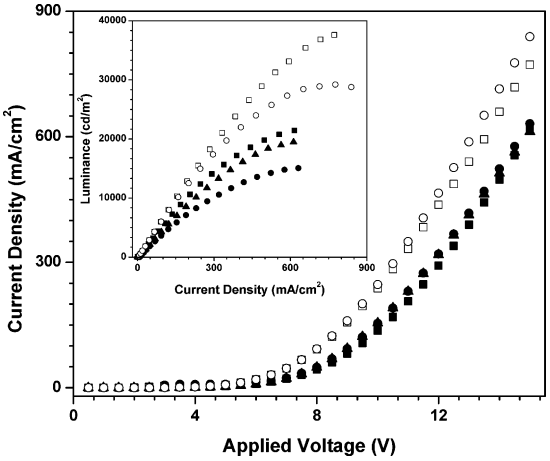

Figure 4. Electroluminescent characteristics for devices containing Alq_3 as the electron-transport layer (legend: ▲ (**2**), ■ (**3**), □ (**4**), ● (**5**), and ○ (**6**)).

Characteristics of Organic Light-Emitting Diodes. Although the molecules described in this paper possesses both electron-donating carbazole and electron-withdrawing oxadiazole moieties, inspection of the HOMO and LUMO (Table 1) energy levels derived from the cyclic voltammetry and absorption edge data clearly underlines that they are capable of functioning as hole-transporting (HTL) agents. Although the molecules also carry an electron-transporting moiety of oxadiazole, the large barrier (1.3−1.5 eV) for electron injection from the cathode to the layer may ultimately affect the performance. So two types of devices using these materials as HTL were fabricated: (I) ITO/**2**−**6** (40 nm)/TPBI (40 nm)/Mg:Ag; (II) ITO/**2**−**6** (40 nm)/Alq_3 (40 nm)/Mg:Ag. Two different electron-transport materials, Alq_3 and TPBI, were used. The device structure and the energy level alignment of the materials involved are displayed in Figure 3. The performance characteristics of the EL devices fabricated in this study are enumerated in Table 2, and I−V−L trends are displayed in Figures 4 and 5.

The EL spectra observed for devices I in general resemble the PL spectra of the vapor deposited film samples prepared under identical device fabrication conditions (Table 2), indicating that the excitons are effectively confined within the HTL layer. A slight blue shift relative to the corresponding PL spectra is observed in the EL spectra of devices I comprising the CF_3

Table 2. Electroluminescent Data for Devices I and II

	1[b] TPBI/Alq_3	**2** TPBI/Alq_3	**3** TPBI/Alq_3	**4** TPBI/Alq_3	**5** TPBI/Alq_3	**6** TPBI/Alq_3
turn-on voltage, V	3.0/3.0	3.0/3.0	3.0/3.0	3.0/3.0	3.5/3.5	3.0/3.0
max. brightness, cd/m^2	40 300/ 30 400	24 740/ 19 460	15 565/ 21 425	36 930/ 37 600	13 625/ 15 065	23 680/ 29 190
max. ext. quantum eff., %	5.2/1.8	2.7/1.5	3.1/1.8	3.9/2.1	2.6/1.8	3.7/2.5
max. current eff., cd/A	10.3/5.7	7.0/4.6	6.8/5.4	11.0/6.6	4.9/3.9	8.8/6.5
max. power eff., lm/W	6.3/1.7	3.5/1.8	2.8/2.0	6.3/2.9	1.8/1.5	4.2/2.9
λ_{film} (fwhm), nm	490	508 (82)	494 (80)	512 (84)	474 (78)	496 (82)
λ_{EL} (fwhm), nm	482 (74)/ 518 (92)	496 (78)/ 510 (88)	486 (74)/ 510 (96)	502 (80)/ 510 (82)	476 (78)/ 482 (86)	490 (74)/ 494 (78)
CIE, *x*, *y*	0.16, 0.29/ 0.28, 0.52	0.19, 0.43/ 0.25, 0.52	0.16, 0.34/ 0.25, 0.49	0.21, 0.47/ 0.26, 0.53	0.16, 0.26/ 0.18, 0.32	0.17, 0.38/ 0.20, 0.42
voltage,[a] V	8.5/9.9	10.33/9.11	10.7/9.4	9.7/8.1	10.4, 9.1	10.2/8.1
brightness,[a] cd/m^2	9630/5270	6000/4530	6030/5370	9780/6550	4915/3900	7610/6450
ext. quantum eff.,[a] %	4.8/1.7	2.3/1.5	2.7/1.8	3.5/2.1	2.6/1.8	3.2/2.5
current eff., cd/A	5.7/5.3	6.0/4.5	6.0/5.4	9.8/6.5	4.9/3.9	7.6/6.5
power eff.,[a] lm/W	3.6/1.7	1.8/1.6	1.8/1.8	3.2/2.5	1.5/1.3	2.3/2.5

[a] At a current density of 100 mA/cm^2. [b] From ref 17.

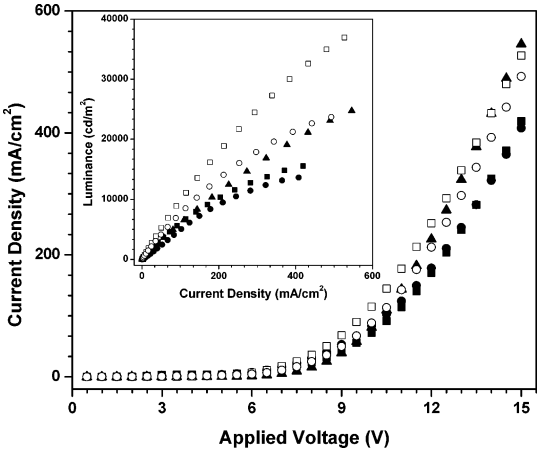

Figure 5. I–V–L curves for devices containing TPBI as the electron-transport layer (legend: ▲ (**2**), ■ (**3**), □ (**4**), ● (**5**), and ○ (**6**)).

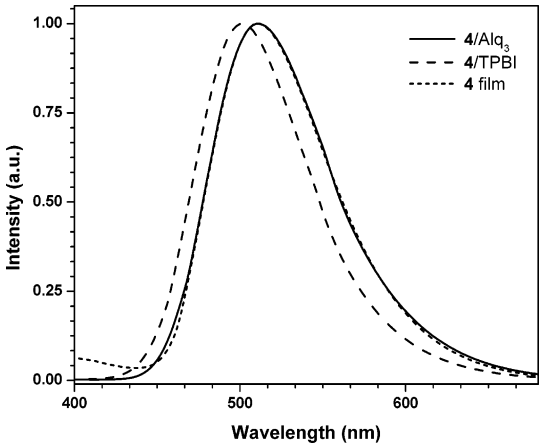

Figure 6. EL and film PL spectra of compound **4**.

derivatives (**2**, **4**, and **6**). A representative illustration is provided in Figure 6. This may be a result of exciplex and/or electroplexes between TPBI and the CF_3 derivatives. In device I, the HOMO energy difference between the HTL and the ETL (1.1–0.9 eV) is significantly greater than the LUMO gap (0.5–0.3 eV). Therefore, holes can be effectively confined inside the HTL layer.

For device II, the energy gap between the HTL and the ETL is closer or even somewhat smaller for the HOMO (0.9–0.7 eV) than the LUMO (1.1–0.9 eV). Consequently, it is possible for excitons to form inside both HTL and ETL. The emission wavelengths of the compounds **2**–**6** are close to that of Alq_3, and unambiguous assignment of the origin of the EL spectra is difficult. However, on the basis of the comparison of the film PL spectra and the EL spectra and the fwhm (full-width at half-maximum), emission in the Alq_3 devices of **4** and **6** likely stemmed from the HTL layer (Figure 6). The Alq_3 devices of **2** and **5** may have a slight emission contribution from the ETL layer. This is also supported by the notable red shift observed for the EL spectra (Figure 7). On the contrary, light emission mainly comes from the ETL layer in the Alq_3 device of **3**. The observation that the majority of EL emission is from HTL in devices II may also be due to a retardation of hole-transporting inside the HTL layer (vide infra). The LUMO energy gap between the HTL and ETL also

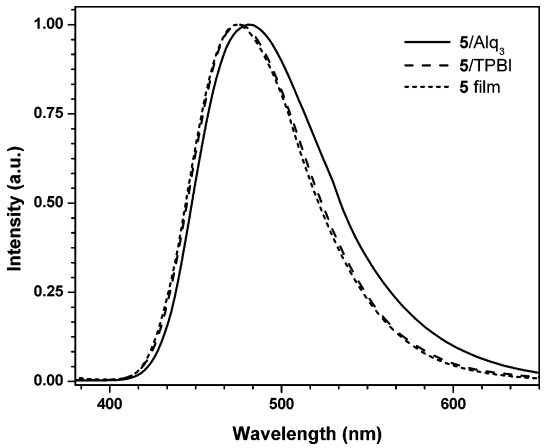

Figure 7. EL and film PL spectra of compound **5**.

plays an important role in determining the exciton-confinement region by blocking the holes. Similar to compound **1**,[17] we reported earlier that **3** also has a larger LUMO gap with ETL. In contrast, the LUMO energy gap between compound **6** and ETL is the smallest among all.

To clarify the contribution of Alq_3 emission in some devices II, we also fabricated devices III of structure ITO/**3** (40 nm)/BCP (10 nm)/Alq_3 (30 nm)/Mg:Ag (BCP = 2,9-dimethyl-4,7-diphenyl-1,10-phenanthroline), where BCP (HOMO = 6.4 eV, LUMO = 2.9 eV)[25] was used as the hole-blocking layer. Indeed, the EL spectra of device III are superimposable with the film PL spectra of **3**. The performance of device III (at 100 mA/cm^2: **2**, brightness = 6519 cd/m^2, external quantum efficiency = 2.3%, current efficiency = 6.5 cd/A, power efficiency = 2.3 lm/W; **3**, brightness = 7425 cd/m^2, external quantum efficiency = 3.3%, current efficiency = 7.4 cd/A, power efficiency = 2.3 lm/W; **4**, brightness = 8735 cd/m^2, external quantum efficiency = 3.2%, current efficiency = 8.8 cd/A, power efficiency = 3.4 lm/W; **5**, brightness = 7605 cd/m^2, external quantum efficiency = 4.1%, current efficiency = 7.6 cd/A, power efficiency = 2.4 lm/W; **6**, brightness = 8553 cd/ m^2, external quantum efficiency = 3.5%, current efficiency = 8.6 cd/A, power efficiency = 2.5 lm/W) appears to be better than that of device II. Compounds containing 2,5-disubstituted 1,3,4-oxadiazole units have been demonstrated to be excellent electron-transport materials.[6b,26] We found that the electron-deficient oxadiazolyl moiety in **2**–**6** retarded the hole mobility in these molecules. For instance, bilayer devices of the structure ITO/**3** (x nm)/Alq_3 (y nm)/Mg:Ag ((a) x = 10 nm, y = 70 nm; (b) x = 40 nm, y = 40 nm; (c) x = 70 nm, y = 10 nm) were fabricated and tested. The current–voltage plots (Figure 8) showed that the total current density decreased in the order of (a) > (b) > (c). Thus, a device composed mainly of Alq_3 layer gave higher current than a device composed mainly of compound **3**; this would imply that the hole mobility in **3** is significantly lower than the electron mobility in Alq_3. We anticipate that

(25) Baldo, M. A.; Thompson, M. E.; Forrest, S. R. *Pure Appl. Chem.* **1999**, *71*, 2095.
(26) (a) Adachi, C.; Tsutsui, T.; Saito, S. *Appl. Phys. Lett.* **1990**, *56*, 799. (b) Adachi, C.; Tsutsui, T.; Saito, S. *Appl. Phys. Lett.* **1990**, *57*, 513. (c) Tokuhisa, H.; Era, M.; Tsutsui, T.; Saito, S. *Appl. Phys. Lett.* **1995**, *66*, 3433. (d) Antoniadis, H.; Inbasekaran, M.; Woo, E. P. *Appl. Phys. Lett.* **1998**, *73*, 3055.

Table 3. Electroluminescent Data for Devices IV

	2	3	4	5	6
turn-on voltage, V	3.2	3.2	3.2	3.2	3.2
max. brightness, cd/m^2	85 207	42 734	81 365	42 734	69 293
max. ext. quantum eff., %	4.3	5.3	4.3	4.3	5.3
max. current eff., cd/A	12.1	12.6	13.2	8.9	13.9
max. power eff., lm/W	6.1	5.9	5.6	3.7	7.6
λ_{EL} (fwhm), nm	504 (84)	496 (82)	512 (80)	486 (80)	500 (80)
CIE, x, y	0.22, 0.48	0.20, 0.40	0.24, 0.54	0.16, 0.31	0.19, 0.45
voltage,[a] V	8.4	9.2	8.5	9.0	9.5
brightness,[a] cd/m^2	11 957	11 468	13 009	8607	12 990
ext. quantum eff.,[a] %	4.3	4.8	4.3	4.2	4.9
current eff.,[a] cd/A	12.0	11.5	13.0	8.6	13.0
power eff.,[a] lm/W	4.5	4.0	4.8	3.0	4.3

[a] At a current density of 100 mA/cm^2.

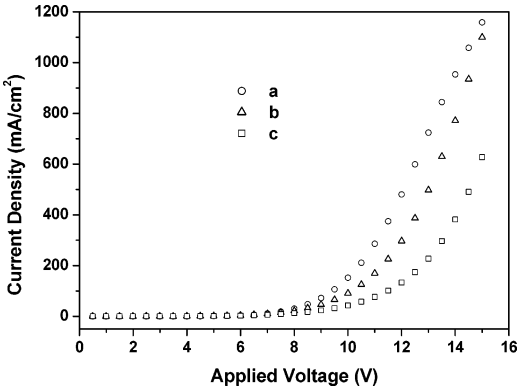

Figure 8. Current−voltage characteristics for bilayer devices of the structure ITO/**3** (x nm)/Alq_3 (y nm)/Mg:Ag ((a) x = 10 nm, y = 70 nm; (b) x = 40 nm, y = 40 nm; (c) x = 70 nm, y = 10 nm).

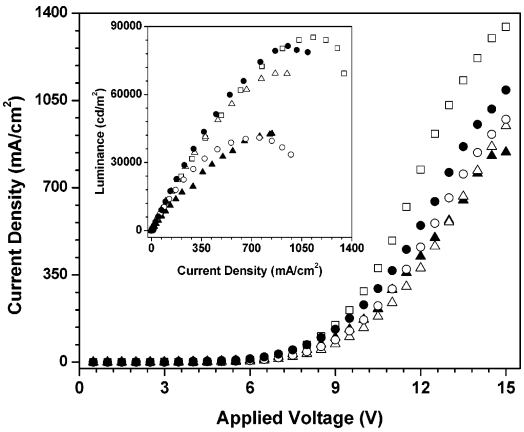

Figure 9. I−V−L curves for devices IV (legend: □ (**2**), ○ (**3**), ● (**4**), ▲ (**5**), and △ (**6**)).

insertion of a better hole-transporting layer between ITO and **2**−**6** will be beneficial to improving the device performance. Therefore, NPB having hole mobility 1 order higher than the electron mobility of Alq_3 was used.[27] Devices IV of the structure ITO/NPB (40 nm)/**2**−**6** (30 nm)/BCP (10 nm)/Alq_3 (30 nm)/Mg:Ag (NPB = 4,4′-bis{*N*-(1-naphthyl-*N*-phenylamino)biphenyl) were fabricated and tested. The performance parameters of devices IV are collected in Table 3, and I−V−L characteristics are displayed in Figure 9. Devices IV appear to have very impressive performance apparently due to a better balance of electrons and holes. Devices of similar structure but with a thinner layer of **2**−**6** have

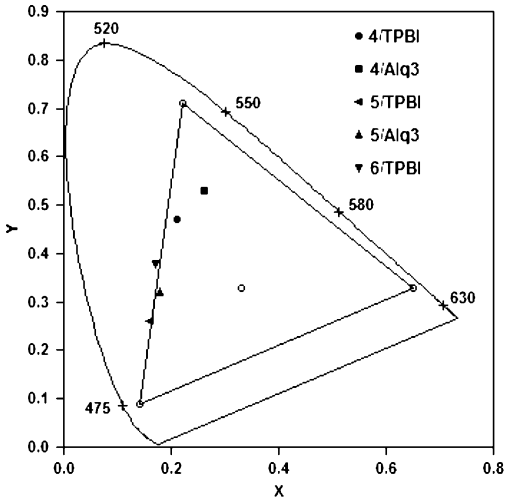

Figure 10. CIE 1931 x, y coordinates plot for representative devices.

inferior performance as compared to devices IV, although the performance still surpasses that of devices II.

In general, the CF_3-substituted derivatives exhibit slightly better performance than the *tert*-butyl analogues, and compound **4** excels in terms of brightness and external quantum efficiency. The improved performance for the CF_3-substituted derivatives could be ascribed to the hole-blocking and electron-transport property imparted by the fluorine atoms.[28] However, color coordinates of most of the devices do not match those of standard primary colors (Figure 10). Instead, they fall between blue and green standards, and thus are better described as cyan. It must be noted here that the molecules possessing primary color (blue, green, or red) emission are necessary for the manufacture of the displays. Nevertheless, the performance of many compounds described here rivals the compounds reported in the literature with similar structural design. These materials may be suitable for device engineering studies leading to white light OLEDs and can also be used as hosts for low-energy emitting materials or triplet emitters.[29]

(27) Strohriegl, P.; Grazulevicus, J. V. *Adv. Mater.* **2002**, *14*, 1439.

(28) (a) Okumoto, K.; Shirota, Y. *Chem. Mater.* **2003**, *15*, 699. Okumoto, K.; Shirota, Y. *Appl. Phys. Lett.* **2001**, *79*, 1231. (b) Heidenhain, S. B.; Sakamoto, Y.; Suzuki, T.; Miura, A.; Fujikawa, H.; Mori, T.; Tokito, S.; Taga, Y. *J. Am. Chem. Soc.* **2000**, *122*, 10240.

(29) Brunner, K.; van Dijken, A.; Borner, H.; Bastiaansen, J. J. A. M.; Kiggen, N. M. M.; Langeveld, B. M. W. *J. Am. Chem. Soc.* **2004**, *126*, 6035.

In summary, we have synthesized a new series of carbazole−oxadiazole conjugates suitable for application in organic light-emitting diodes. Incorporation of electron-withdrawing substituents such as CN and CF_3 affects the emission, thermal, and electronic properties of the compounds. A slight modification in the structure leading to reasonable alteration either in luminescence maximum or in HOMO is attractive and will be useful in the future design of functional materials for specific purpose.

Acknowledgment. We thank Academia Sinica and the National Science Council for financial support.

CM048794U